Journal of Interdisciplinary Mathematics
ISSN: 0972-0502 (Print), ISSN: 2169-012X (Online)
Vol. 27 (2024), No. 7, pp. 1531–1552
DOI : 10.47974/JIM-1905

A topological and 3D-geometrical study about an initial skeleton of the 2MASS Pleiades nucleus with DR2 distances

F. J. Marco Castillo *
Departamento de Matemáticas
Instituto Universitario de Matemáticas y Aplicaciones de Castellón (IMAC)
Universitat Jaume I
Castellón 12071
Spain, España

M. J. Martínez Usó †
Departamento de Matemática Aplicada
Instituto Universitario de Matemática Pura y Aplicada (IUMPA)
Universitat Politècnica de València
Valencia 46022
Spain, España

J. A. López Ortí §
Departamento de Matemáticas
Instituto Universitario de Matemáticas y Aplicaciones de Castellón (IMAC)
Universitat Jaume I
Castellón 12071
Spain, España

Abstract

The appearance of successive versions of the Gaia Data Release has prompted the realization of many works on the Pleiades, whose objectives range from the identification of new stars to the study of the cluster dynamics. Our study has a different focus, although we start by identifying a subset by imposing geometric restrictions on the m45 file from the Gaia website itself. We consider only the 2MASS stars in the file and use the stellar distances adopted in EDR3, applying restrictions concerning a high density in the spatial distribution and small distances between stars. With this denser nucleus, we carry out a study of the three-dimensional point cloud with Topological Data Analysis (TDA) techniques. We investigate its topological and geometrical structure using two TDA methods that provide

* *E-mail:* **marco@mat.uji.es (Corresponding Author)**
† *E-mail:* **mjmartin@upv.edu.es**
§ *E-mail:* **lopez@mat.uji.es**

different results. To clarify this problem, we introduce a dual method over a net of points where null densities are obtained and will be used to discuss loops and voids. Also, two connected components are found, and finally, we will relate the astrophysical properties of these stars for each connected component with the deduced topological-geometrical results. The small set can subsequently be expanded with stars from DR2, not 2MASS.

Subject Classification: *(2010) 62-07, 85A15.*

Keywords: *Topological data analysis, Astronomy, Open clusters, Pleiades.*

1. Introduction

Our goal in this paper is to conduct an introductory and prospective study about the possible interrelationships between the topological-geometrical structure of the Pleiades nucleus (in a range of magnitudes limited by the values provided by the 2MASS catalogue [4] and [12]) and the available data concerning proper motions and some astrophysical properties. The initial positions, right ascension and declination, are taken from 2MASS, and the rest of the data from DR2 [5], the second Data Release of the Gaia project, including the heliocentric distances assigned to each star [1] and [6], required to consider a three-dimensional problem.

There are already studies in which TDA techniques [2], using different pacages such as GUDHI [9], are applied to astronomical data, but they consider large space areas with corresponding huge distances. Such are the cases, for example, of the articles about the Cosmic web [13] or the study of molecular filaments in our galaxy [11]. It is evident that to apply the information from these papers to a smaller area in our galaxy a simple zoom would be meaningless. Different scales require different treatments for the problems.

Going into detail about the reason for considering the Pleiades cluster is unnecessary. We will just point out that regarding problems of galactic distances [16] or stellar evolution [3], the better the knowledge about them, the more we can advance in solving more ambitious problems.

There are so many papers about different issues regarding the Pleiades open cluster that it would be presumptuous to pretend to summarize all of them. Instead, we will limit ourselves to saying that, although it may seem strange, how many stars constitute the cluster mentioned above has yet to be precisely known. Indeed, there is a greater consensus about the extension of the nucleus and the inner nucleus. However, these last concepts should also be clearly defined, although we can roughly relate them to a more or less high density in the concentration of stars. Our initial file, based on the distances taken from the Bailer Jones et al. [1] and incorporated into DR2 and EDR3 [6], was a file obtained from Vizier [14] called "Pleiadest", where more than 70,000 stars (only in right ascension and declination) are given with 2MASS positions and also contained in the Tycho-2 catalog [7]. This file evidently contained stars that are indeed from the Pleiades but also others called field stars which, by definition, do not belong to the cluster but must be differentiated from those that do belong. The classical procedures to discern which ones can be considered as belonging to the cluster and which are field stars make use of specific astrophysical properties of the stars (note that in these works, distances are not considered so that the field stars and those of the cluster of the Pleiades are in the plane tangent to them and it is impossible, if not by complementary methods, to distinguish them). It is no longer surprising that there are as many different cluster proposals as authors. It is also worth noting that the kinds of magnitudes chosen in each research can modify the results. For this reason, Gaia's higher range of magnitudes can allow completing or modifying results obtained only with observations on the celestial sphere (only with right ascension and declination, as in the case of 2MASS). However, as this paper is part of a broader study in which our objective will be the correction of 2MASS[1], we have focused on the small set of the Pleiades and, in particular, on an even smaller subset, the densest nucleus. This process of reduction in the data selection will be evident during the exposition since it is a consequence of the results obtained and the respective star selection criteria.

In the next section, we consider a first step, based on geometric data, to reduce the initial set of points. An ideal 3D-position of the geometric center of the cluster will be found, and a spatial vision will be given. It may be helpful to have a view of the cluster with respect to the planes associated with the principal components analysis (PCA) of the data set to see the geometry intrinsic to the cluster. The equatorial plane stands out among the coordinate planes, so it is convenient to identify it. This plane divides the cluster into two hemispheres, one upper and one lower, which are intrinsically connected to the geometric structure of the cluster. However,

[1] The final corrected 2MASS catalog will be transformed into the DR2 system with the proper motions that this latter catalog provides. Later, these corrected positions will be compared with the 2MASS positions given by DR2. Assuming that DR2 proper motions were accurate, we hypothesize that the difference between the two set of positions is due to the terrestrial 2MASS observations.

working with a distribution of points referred to the resulting PCA planes is unnecessary, although we may use this in later studies.

A simple visual inspection of the cloud of points allows us to see "almost" two connected components of the considered set. We verified that by artificially removing 24 stars, this becomes evident. Of the two connected components, we will stay with the one that contains the most stars, relegating the study of specific physical parameters in both components to the final part of the work. Regarding the main connected component, we will conduct a simple TDA study using two different procedures to highlight an existing problem for clouds of points in general, including the one in this work.

A subsequent study, which we call dual, based on the points of a grid to which a null density can be associated, will allow us to open two ways of examining the problem in more depth. On the one hand, the partial visualization for a better vision of the topological structure of a zone of the nucleus (in fact, only loops and voids, ignoring the connected components) by means of an alpha complex study, computing Betti numbers depending on the value of the alpha parameter of the filtration in which we stop the procedure. The second idea, which will not be developed here, is approaching a structure in two ways, the direct and the dual, until they differ by an admissible distance.

In Section 4, we will see certain graphs on density distributions of astrophysical parameters, their distributions as a function of the distance to the center of the nucleus, and HR-type diagrams that may point to some relevant properties and which can be connected to some previously determined topological properties. Finally, we give an explanation about the null influence in this study of the artificial elimination of the 24 stars apart from the correct determination of two conected components

Summing up, this paper is structured in three sections:

1. Discussion about data selection.
2. Topological analysis of the nucleus of the Pleiades and its difficulties. A proposed approach to a satisfactory resolution of the problem through the use of a dual approach.
3. Search for relationships between the selected astrophysical data and the topology of the Pleiades. The relationship between the physical data, the loops and the void obtained in Section 3 will be dealt with in a further paper, in which the proper motions will also be considered in detail. Here we will only focus on the differences, more or less

evident, between the two connected components that seem to exist and the chosen astrophysical data.

4. We conclude that removing the 24 stars does not influence the studies carried on in Section 4.

2. Data selection

We have started with a file from the Gaia web page, gea.esac.esa.int/archive, provided by means of a search using the keyword m45 or Pleiades. This initial file contains 108762 stars, which is clearly an excessive number of elements: Only a few must be stars of the Pleiades, and the remaining are field stars. In the subsequent steps, the heliocentric distances have been taken, in parsecs, from Bailer-Jones et al. [1] (distances incorporated into DR2 [5] and EDR3 [6]) to have the spatial coordinates of each selected star. At this time, we are in a position to apply metric criteria to restrict ourselves to the inner nucleus of the cluster.

From the initial file, we are left with only those stars located at a maximum distance of 600 pc from the Sun. We accept as heliocentric distance to the cluster's center the value r = 136 pc, provided by Gaia DR2 (it is noteworthy that there is more than 10 pc difference with the estimate

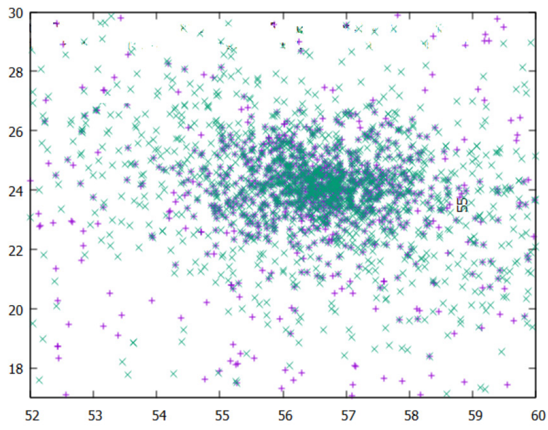

Figure 1

Initial 2D distribution of the stars employed in the paper in violet and those chosen by Lodieu et al. [8] in green. As can be seen, the cluster's shape does not change no matter which set of stars we choose. Our sample has been obtained from the approximate geometric center of the initial 2556 stars. The 3D center is located at (68, 102.5, 53.7)

previously provided after the Hipparcos mission). Studies carried out after the publication of the EDR3 data suggest a cluster radius of around 10 pc. Thus, we create a new file with those stars whose heliocentric distances are in a range between 120pc and 150pc. This new file contains 2556 2MASS stars and provides a fiducial center at the point of heliocentric equatorial coordinates (68.1, 102.4, 53.1). The point, in 2D-equatorial heliocentric coordinates is (AR, DEC) = (56.6º, 23º). In order to compare the state of the results, up to now, the stars obtained have been projected onto the celestial sphere and compared with those obtained (in 2D) by Lodieu et al. (2281 DR2 stars, in total) [8]. Both sets of stars can be seen overlapped in different colors in Figure 1. This catalog of 2281 stars can be obtained from Vizier (J/A+A/628/A66/pleiades), and it was uploaded to this site after we independently carried out our own determination of positions, so Figure 1 is quite representative of the similarity of the sky area covered by their data and ours.

Two issues should be highlighted here: a) this obtained point is fiducial, and although we refer to it as the center of the cluster, it does not really represent its center of gravity: To obtain this, many more refinements are needed, including determining all the stars in the cluster, their relative positions, and their assigned masses. This issue is largely out of the objectives of this study; b) given that we want to carry out a geometric and topological study and try to relate it to specific values of its physical parameters, the study is intrinsic to the cluster shape and does not depend on the reference except, perhaps, a translation in the variable r that represents the distance to the chosen center: the structure of the whole set remains unchanged in all its aspects.

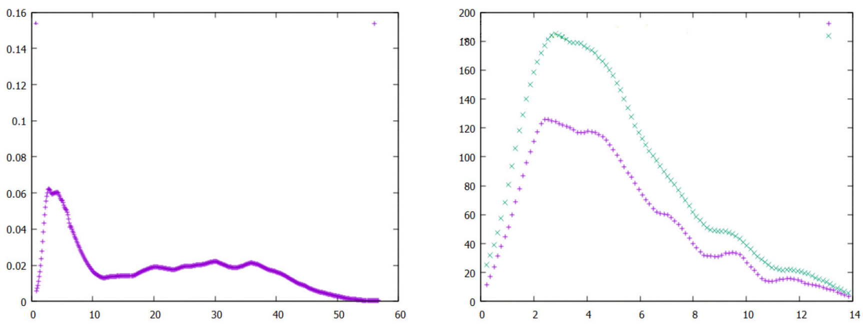

Figure 2

Figure 2a (left) density distribution plot of the distances to the cluster's center. Figure 2b (right) non-normalized density with bandwidths h=0.8 and h=1.2

Likewise, once a center has been chosen, it is possible to find the probability density function (pdf henceforth) of the spatial distribution, depending on the stellar distances to that center. To this aim, we take a slightly larger set than the last already found in order to ratify or not, beyond the contrast with Lodieu's stars seen in Figure 1, the choice of a nucleus radius of 10 pc. We denote this specific nucleus as the external nucleus of the cluster. This previously mentioned density function can be observed in Figure 2a, where we can see that the highest densities are found up to a distance of between 10 – 12 pc from the center. In addition, approximations by non-normalized kernel pdf, with bandwidths h=0.8 and h=1.2, can be seen in figure 2b). Subsequently, there is another set of stars, up to a distance of about 40 pc from the center, with a lower density and that can be used to study the stars that are outside the cluster nucleus, including stars that are in the process of escaping from it. We are not going to carry out this type of study here either, so we are left with the stars that are at a distance from the Sun, between 120 and 150 pc, and that, depending on the center and the radius, we can frame in the cube [60, 80]x [95, 115] x [45, 65], all heliocentric distances in pc. In order to narrow more accurately the inner nucleus, understood as the place of the greater density of stars, we consider a subset of stars with the property that each of them has some other star at a distance less than or equal to one pc. We are finally left with a set of 1005 2MASS stars, with which we will work in the rest of the paper and which represent the 2MASS stars found in what we will call the inner core of the cluster. Figure 3 consists of the three-dimensional representation of the set of stars in the selected cube and where specific orientations have been chosen for the purpose of visualization of certain geometric structures. On the left, without the restriction of the existence of another star at a distance less than or equal to 1 pc, and on the right with that restriction. However, it can be globally seen in Figures 3a and 3b that the structure remains unchanged. The resulting set has its barycentre at (68, 103.1, 55) with units in pc. The displacement of 2 pc between this point along the z-axis and the one found with the 2556 stars determines a 2D position for the center given by (AR, DEC)= (56.6º, 24º) where there is a variation of only one degree in the declination. See the comment in the following paragraph on the effect of this difference.

Visually, we can highlight some particularity from these three-dimensional graphs in Figure 3. Some details can be seen in these spatial distributions, such as the fuzzy defined nucleus, leaving many isolated stars. It is also observed, around the center of the figure, what could be a tunnel, with an associated loop, over the center of the figure. Finally, it can be observed that a low density of stars separates two zones. We will see that, indeed, by artificially removing this small number of stars (we have removed 24), two connected components clearly appear (see Section 3). This artifice is made to study if these two components (considered almost artificially) have differences in some physical parameter. To do this, we will wait until section 4.

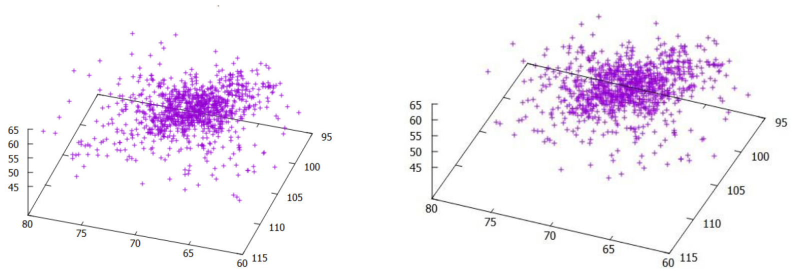

Figure 3

Two different views of the nucleus of the Pleiades with different orientations where some topological features may be intuited. Figure 3a (left) contains 2556 stars. Figure 3b (right) contains 1005 stars.

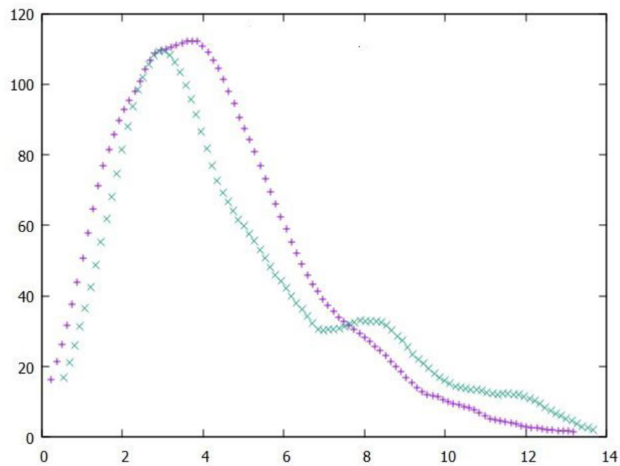

Figure 4

The pink (non-normalized) graph corresponds to the upper hemisphere and the green to the lower. An asymmetry is observed in the maximum concentration of stars for both hemispheres: the upper one close to 4pc and 3pc for the lower one. A concentration is also observed, more accentuated in the lower hemisphere, around 8 pc.

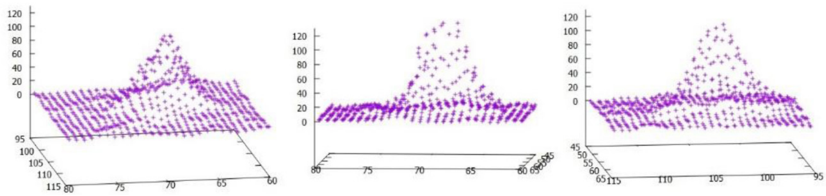

Figure 5

3D projections on the coordinate planes of the actual graph, which is in 4D of the estimation of the density function as a function of the heliocentric equatorial coordinates. A visual inspection corroborates the simple conclusions about the cluster geometry that have already been intuited.

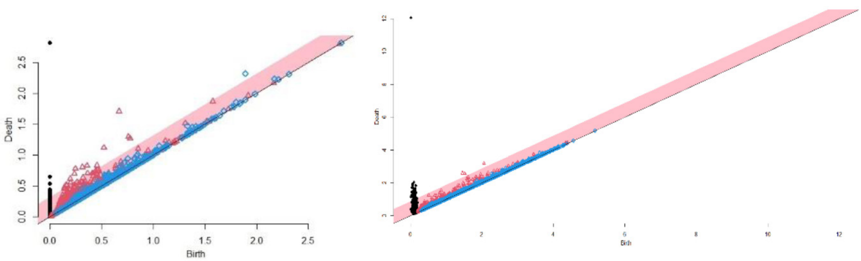

(a) **(b)**

Figure 6

We can appreciate that, on the right-hand side of 6a), a void appears, while on 6b), it is not detected. As for the loops, three appear using the SCHU method, and some more using the alpha shape. See explanation in text.

3. Topological analysis of the nucleus of the Pleiades and its difficulties. Proposal for approaching the problem

Firstly, to better visualize the geometric distribution intrinsic to the cluster, we proceeded to orient the cluster according to the axes resulting from applying the Principal Component Analysis method. Once the change of coordinates has been made, we have split the two resulting hemispheres with respect to the component that marks the cluster's equator. A density function for each hemisphere has been obtained for the stars' distances to the cluster's center. We can see it in Figure 4, in which the pink graph corresponds to the density corresponding to the upper hemisphere and the green to the lower. An asymmetry is observed in the maximum concentration of stars for both hemispheres: the upper one close to 4pc and 3pc for the lower one. A concentration is also observed, more accentuated in the lower hemisphere, around 8 pc.

We have also computed the density for the spatial distribution and the marginal densities with respect to the sets of variables xy, xz, and yz from equatorial heliocentric coordinates. Due to the impossibility of graphing the density, we have tested, for example, the partial density with respect to the xy variables and then its projection onto the planes XY, XZ, and YZ (see Figure 5). It should be noted that these marginal densities have been made for the initial set of 2556 stars and in the heliocentric position. However, we would get the same result working with the 1005 stars selected later and even obtaining the marginal densities with respect to the axes determined by the main components and with the origin of coordinates in the center of the cluster. These figures are in complete agreement with the general properties concluded from a kernel density study regarding distances to the center. Nevertheless, we have more detailed information about the true position of the peak signals in the more superficial analysis.

Once a global study of the geometric structure of the cluster has been carried out, we will move on to the topological study of the cloud of points that represent the stars. First, two persistence diagrams have been obtained by means of two different procedures. Both of them have been applied over the set of 1005 stars, eliminating the 24 mentioned. The first is through an alpha complex method (Figure 6a), and the second is from a Voronoi cells approach after a kernel smoothing application with a bootstrap band estimation (SCHU method, from Xin Xu [15]) (Figure 6b). The bandwidth of the alpha method has been taken similar to that obtained by bootstrap. The difference in loops and voids is clear, and we think that this is due to an over-smoothing in the second method. This issue will be discussed in more detail below. We can appreciate that, on the right-hand side of Figure 6a a void appears, while in Figure 6b it is not detected. As for the loops, three appear using the SCHU method, and some more using the alpha shape method. Regarding the way of expressing the connected components, there is also variation, although in Figure 6a we can see that there were two originally. It is more complicated to see details in Figure 6b, probably due to the scaling used by the calculation routines. Let us intuitively discuss the problems arising from using the two different procedures. To do this, in the following subsections, we will add to what has been done so far with complementary approaches to each problem.

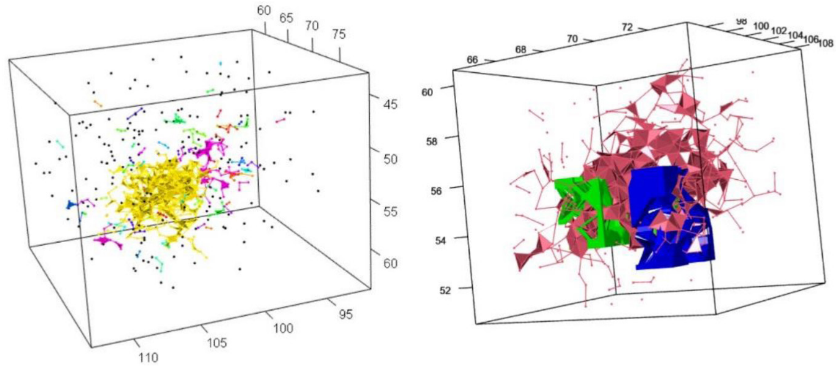

Figure 7

Connected components (left) and loops (right)

3.1 *Connected components*

We recall that both approaches to persistence diagrams have been obtained from the original 1005 stars set where 24 stars have been eliminated, as previously stated, to clarify the variation in the stellar distribution in space. The alpha-shape with alpha=0.45 provides Figure 7 (left), where only two connected components are significant. One with 660 stars and the other with 61 stars. We will denote them as cc1 and cc2, respectively. Different procedures have been tried to obtain absolute isolation of such components. This has yet to be achieved in a completely satisfactory way, and for this reason, we do not insist more on this issue that will be the subject of a more in-depth review in the future. However, we include a final section with a brief discussion of the implications of these 24 stars in the obtained result and we conclude that eliminating them or not is irrelevant for the studies collected in Section 4.

3.2 *loops*

Just as in studying connected components, we can try to attribute gravitational causes to their existence. In a real situation like ours, explaining what a loop represents and, much more, visualizing it geometrically is always challenging. Given the two persistence diagrams that are as different in the H1-generators as those presented previously seen in Figures 5a and 5b, we propose a complementary approach to try to find the significative differences between them. Specifically, we consider a mesh containing the cluster and, once the density function has been calculated, we are left with the set of points of null density computed taking a 3D Epanechnikov model and considering specific bandwidths for each area studied. We anticipate that we have only limited ourselves to two areas, in which loops can be seen). It is evident that a more in-depth study is required: actually, we want to obtain two complementary ashapes that form, approximately, the convex hull of the set. The first ashape is obtained from the stars, and the points of the null density mesh determine the second. In Figure 7 (right), we can see the partial results (an interactive graphic is available in loops.html). It is important to note that the second procedure may be especially useful for tracking tunnels in complicated 3D structures, such as those formed by the clouds of stars that make up the clusters.

3.3 Void

Only one of the persistence diagrams shows a void at the end of the filtering process. We have located it using "cycleLocation" (This information is provided by the "ashape3d" function belonging to the Dionysus package [10]) at the approximate point (66, 102.4, 54.9). A black sphere with a diameter of 0.4 pc has been represented at this place to show its situation in Figure 8. However, at this step the void has yet to be created. When it finally appears in the persistence diagram it will be embedded in the shape and, therefore, invisible (an interactive graphic is available in void.html).

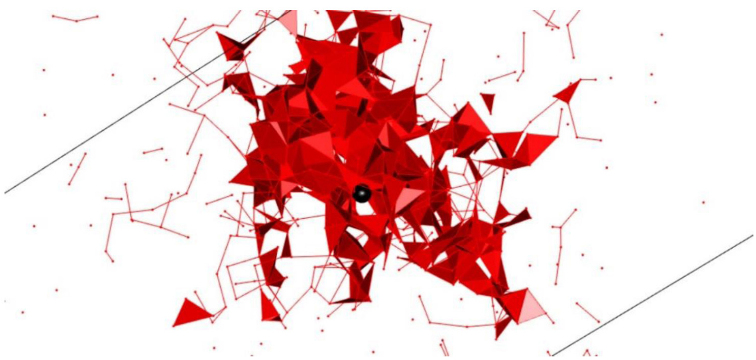

Figure 8

Black sphere of 0.4 pc in diameter whose center is the coordinates of the void mentioned in the text. The initial alpha used to create the ashape is 0.45, but to be able to visualize the ball, it has been necessary to stop at an earlier moment, namely 0.40.

4. Astrophysical data and topology of the Pleiades

The working data, apart from the position in right ascension, declination, and distance, include the proper motions in right ascension and declination (unfortunately, the percentage of stars with known radial velocity is very low), the parallax, the effective Temperature (Teff), Br-Rp color, average magnitude in the G-band (G), from which we deduce, together with the parallax, the visual magnitude; the [Fe/H] concentration, the mass, and the surface gravity (logg). The distance, in parsecs, to the center of the cluster is denoted as r, and cc1, cc2 are the connected components observed. The density functions have been calculated for each selected parameter and for each connected component, as well as the variation with the distance to the center of such parameters and some H-R style diagrams. Let us see in figures 9-15, the graphs with the most notable results.

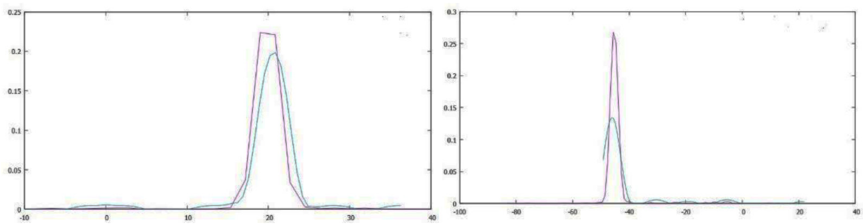

Figure 9

Probability density functions for RA proper motions (left) and dec (right)

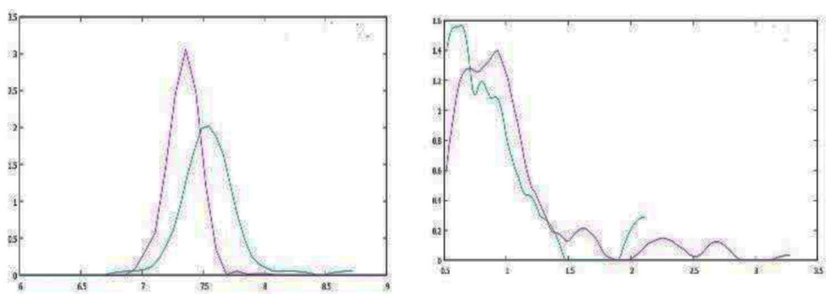

Figure 10

Pdf for parallax (left). Pdf for mass (in solar mass, right) Red stands for cc1 and green for cc2.

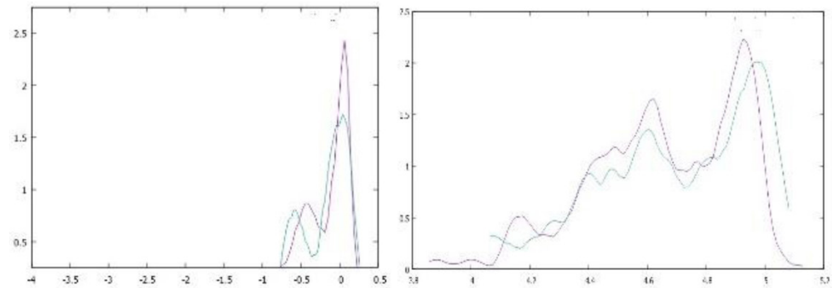

Figure 11

Pdf for the [Fe/H] concentration (left). Density functions for logg concentration (right)

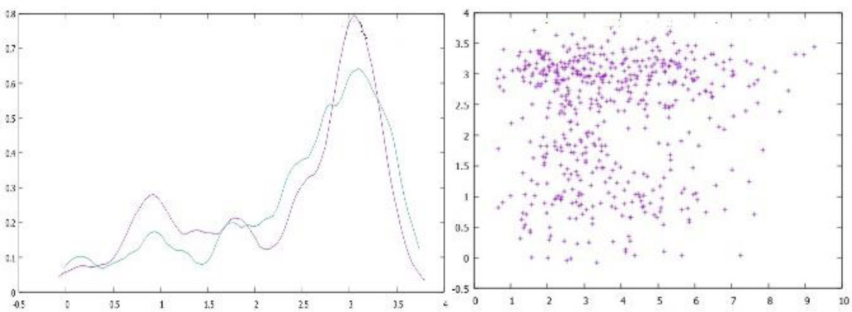

Figure 12

Pdf Density functions for BR-Rp (left). Red stands for cc1 and green for cc2. Distribution in r for the Br-Rp and cc1 (right).

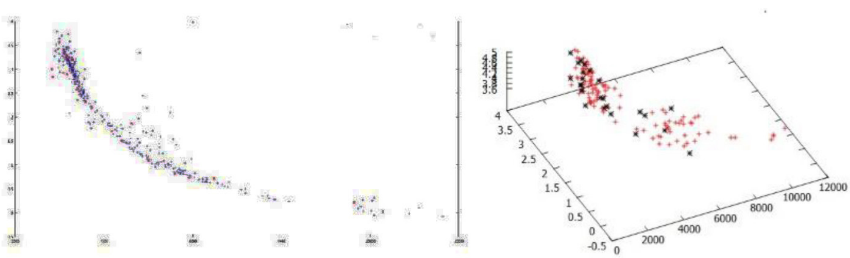

Figure 13

3D graphic for Teff-Br-Rp-r (right), Red stands for cc1 and black for cc2. HR diagram (Right).

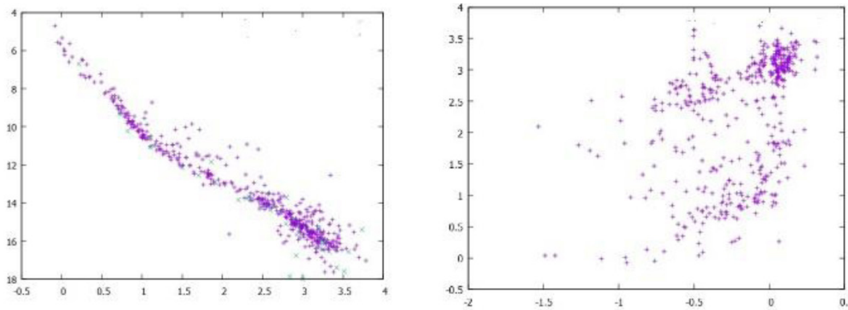

Figure 14

HR diagram (left). Diagram of Fe-H-Br-Rp (right).

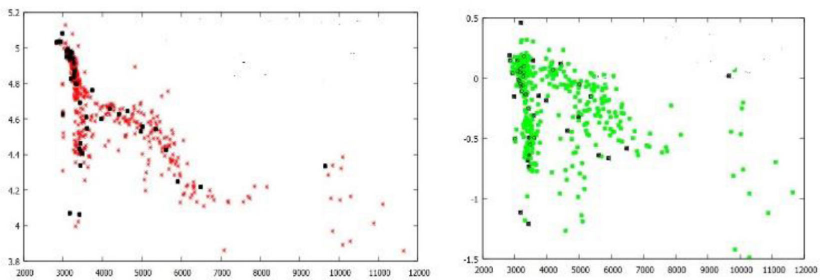

Figure 15

Diagram for Teff-log (leftr) and Teff-FeH (right). Red and green stand for cc1 and black for cc2

From the previous figures, we can deduct some outstanding remarks to this section:

a) There is a shift in the RA proper motions between the components, which is less evident in DEC. A primary mode is present in both ccs, and a secondary mode appears only in cc1. The behavior according to r is increasing for cc1 and decreasing for cc2, just the opposite behavior of parallax. See Figure 9.

b) The star DR2683018727772823552, plx=2.8720, considered an outlier, has been eliminated for parallax. The slopes, according to r, are -0.06 for cc1 (mean 7.3) and 0.07 for cc2 (mean 7.56). See Figure 10a.

c) The average of the masses is approximately 1 solar mass for cc1 and 0.7 for cc2. See Figure 10b.

d) For [Fe-H], the main peak for both ccs appears around zero, and there is a secondary one around -0.5 with a slight displacement between both components. See Figure 11a.

e) For logg, we find two modes in 4.6 and 4.9 for cc1, and 4.6 and 5 for cc2. See Figure 10b.

f) cc1 and cc2 present two common modes at r = 1 and r = 3 for Br-Rp color, and there is an additional mode at r = 1.8 in cc1. See Figure 12 a, b.

The previous remarks are related to our interest in seeing how specific physical parameters are reflected in the spatial distribution of the nucleus concerning the topological and geometrical properties. We could add a more complete analysis offering e.g. studies about the different modes of the pdf relating to the different physical parameters. Another possibility is the study of the different sub figures that appear in the HR-diagrams-type in Figures 13b, 14a,b and 15a,b. The HR-diagram does not show any anomalies and can be found in figure 12a

Finally, radial velocities are essential to launching dynamic simulations in search of hypotheses about the birth and possible evolution of the cluster, but there are too few data to provide conclusive studies.

5. The 24 excluded stars revisited

In sections 3 and 4, geometrical, topological, and physical studies have been carried out without considering 24 stars. In this last section, we briefly deal with some consequences of theis artificial removal. They are located as a separation between the two connected components, so it is reasonable that they have properties closer to one or the other. To see the possible impact of their artificial removal in our study, leaving aside that of the connected components, we have studied how far away each of the 24 stars is from the two connected components. It is immediate to see that if we make a graph (see Figure 16), with the distances to cc1 as the OX axis and the distance to cc2 as the OY axis, there are only three stars that are in a band of amplitude 1 pc and centered on a straight line marking the equidistance of both components. For two of these 3 stars, with respective DR2 identifiers DR2 65223583812996864 and DR2 65201245688454144, none of the physical parameters that we have considered in the study are provided in DR2. For the third of them, that is the closest to cc2 with a distance of 0.565pc, compared to a distance of 0.82 pc to the nearest star of

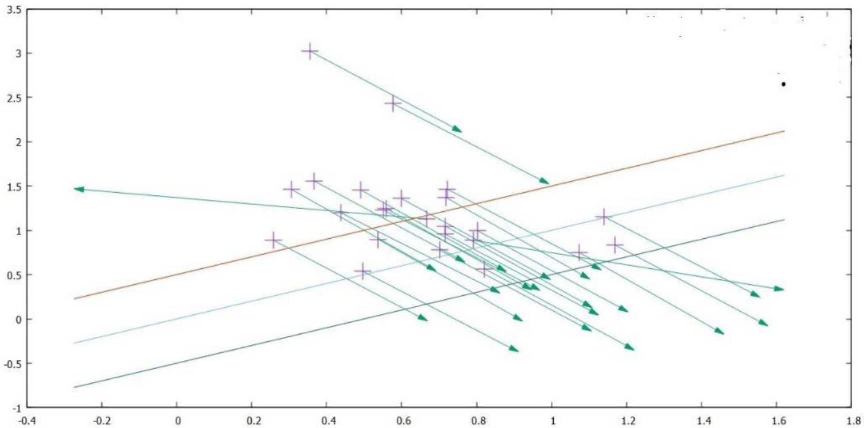

Figure 16

Graphical representation of the distances to cc1 and cc2 of each of the removed 24 stars. A band of 1pc width is added and the vectors represent the normalized proper motions. See text.

cc1, we see that most of the parameters are closer to the values corresponding to the nearest star: concentration [Fe/H], G magnitude, luminosity, zf flux, parallax and proper motion in declination. On the contrary, there are more similarity to the values of the nearest star of cc1, corresponding to the Br-Rp color and the proper motion in right ascension. The rest of the stars are closer to cc1, all of them. In Table 1, we provide each of the 24 stars, together with the stars from cc1 and cc2, closest to them, with their corresponding identifiers and distances. The normalized tangent vectors with the proper motions as well as the radial velocity when this is available, have also been included. Given the scarcity of radial velocities, we have focused only on the normalized tangential velocities that have been represented, showing excellent uniformity except for two stars: one with identifier DR2 65219078390661504 and a direction opposite to the rest, probably be due to a typing error of some sign when compiling the catalog, which does not provide its physical parameters either, and another, with identifier DR2 65230833717683712 that, even following a similar direction, has a low proper motion value, in absolute value, for declination: -11.371 mas/yr and for which no physical parameters are available either.

Bearing in mind that the simplexes have been made with an alpha value = 0.45, these last three mentioned stars are the ones that make it difficult to determine the existence of the two connected components. We can therefore conclude that the study in section 4 is accurate according to the artifice of eliminating such 24 stars since it is immediate to verify that including the 21 stars closest to cc1 does not affect the density properties of the different physical parameters.

6. Conclusions

In this article, we have determined the Pleiades' inner nucleus with stars in the 2MASS catalog. To this aim, we have started from a set of stars obtained from the data provided by Gaia and crossed them with 2MASS. Subsequently, we have considered the distances given by DR2 and, taking into account the position of the center of the cluster and the distance currently accepted to it, a study of the density function of the stars as a function of the distance to the center of the cluster has been carried out. This provides two files, one with distances up to about 45 pc and another up to distances of around 10-12 pc from the center with a high density, which we understand corresponds to the nucleus. Once completed this procedure, a more accurate delimitation was carried out, resulting in a file with 1005 2MASS stars inside a volume of 1000 cubic pc. With this last file, a geometrical study has been carried out using three-dimensional projections of marginal density functions whose graphic representations are four-dimensional when we work with three-dimensional data, having to project onto coordinate planes to obtain, visually, some geometrical information.

Subsequently, and after a simple visual inspection, we observed the existence of loops and two clearly differentiated connected components. However, using the two of the procedures detailed in the text, the topological study of the nucleus has been carried out, applying TDA techniques and obtaining two persistence diagrams. Initially, only one connected component is detected by both methods, showing the difficulty of dealing with point cloud problems of this type. Then, it was decided to artificially eliminate 24 stars in what we could call a kind of channel separating two undetected related components. In one of the studies, a void emerged, while in the other, it has not. In addition to the void, two connected components and several loops have also appeared. Thus, we have investigated along the lines of the first of the two procedures (alphashape3D), and we have tried to locate the indicated void and some of the loops. To this aim, we have introduced a technique, which we have called dual, by computing, for a network of points in the selected cube, those points that have a null value of the estimation of the density function

Table 1

Data of the 24 removed stars.(x,y,z) represent the 3D-equatorial heliocentric coordinates. DR2 is the corresponding identifier of the star in DR2. cc1-dist and cc2-dist are the distance to the nearest stars in cc1 and cc2, respectively. DR2-cc1 and DR2-cc2 are the identifications of these stars. |v| is the module of the velocity. RA pm and Dec pm are the normalized proper motions in RA and dec, respectively. Finally, v_R represents the radial velocity. Null values represent absence of this data.

x (pc)	y (pc)	z (pc)	DR2	cc1-dist (pc)	DR2-cc1	Cc2-dist (pc)	DR2-cc2	|v| (mas/yr)	RA pm	Dec pm	v_R (km/s)
66.8369619061	100.5495038987	54.5224828192	65281166437426176	0.7169181796	65279418387728896	0.9582538742	66798496781121792	49.500	0.409	-0.912	4.96
66.5246035071	100.3401654996	53.4788057871	65217605216685568	0.7158514704	65267078945207296	1.0472583510	65209079706818176	52.008	0.393	-0.919	0.00
66.1016205268	100.4318590692	53.5974356385	65223583812996864	1.0742877123	65267078945207296	0.7515747904	65209079706818176	49.464	0.386	-0.923	0.00
68.5138334714	100.1348910863	56.6202477271	68378563708730624	0.8022576413	68368629448159616	0.9946755797	69889876800977408	51.110	0.402	-0.916	0.00
67.2889259228	100.9935961644	56.8460577528	69834866859848192	0.2586677225	69834759483788928	0.8896518864	69889876800977408	50.778	0.411	-0.912	7.03
68.7420795597	100.3571428726	55.8582031917	68363411064150272	0.7218600305	68368629448159616	1.4635189225	68322454256073344	49.555	0.411	-0.911	0.00
66.5536328686	100.8471003362	53.7556511659	65217222966811264	0.5994690671	65190838982357760	1.3616746599	65209079706818176	47.830	0.398	-0.917	0.00
66.9753632541	100.8342292729	53.2142021892	65178190301724544	0.3662901480	65190838982357760	1.5567370070	65007083101413888	51.014	0.403	-0.915	0.00
67.8997227778	100.4760246037	56.6846159018	69877163697813248	0.4972255961	69829541100441600	0.5385768693	69889876800977408	50.604	0.415	-0.910	0.00
67.1990266888	100.3844571369	54.5162713870	65287458566524928	0.7020612627	65247704349267584	0.7781090854	68295481861500928	49.152	0.404	-0.915	0.00
66.3405135012	100.3106876874	52.9411354890	65201245688454144	1.1696165495	65190838982357760	0.8357310185	65007083101413888	47.923	0.408	-0.913	0.00
66.6680304150	100.1697925667	53.4468691342	65219078390661504	0.6666509257	65267078945207296	1.1278982357	65270450496044416	54.498	-0.940	0.341	0.00
67.4851518237	100.8430279484	56.3525748130	69814388455816960	0.5368067041	69811639676769536	0.8990241677	69878503727603072	52.055	0.386	-0.923	4.05
67.5282332500	100.5058085341	55.8674570253	69811364798863744	0.8207977443	69811639676769536	0.5658711108	68322454256073344	50.040	0.400	-0.917	0.00
66.9003393975	100.7408874818	53.7159995818	65216363971331072	0.3055768877	65195404530870144	1.4621051321	68295481861500928	50.650	0.387	-0.922	0.00
68.4356152864	100.5577846408	55.8680179936	68317609532996480	0.5591775592	68296650092601088	1.2487158995	68322454256073344	50.175	0.388	-0.922	5.51
69.0776870452	102.4900372707	55.7416013241	65289623229979136	0.3552043398	65289588870240384	3.0217460637	69889876800977408	49.624	0.406	-0.914	5.69
67.6715104452	100.6913307880	54.1873490087	65248151025861120	0.5520509133	65247704349267584	1.2316526711	68295481861500928	52.109	0.418	-0.909	16.39
67.9377003479	100.6791053193	54.6414894854	65289004754691200	0.4374190779	65264506261240448	1.1982741643	68298093201624960	49.461	0.425	-0.905	0.00
66.3666729485	100.4875182355	54.1126300953	65230833717683712	0.7920962945	66729635568719872	0.8882507858	66798496781121792	20.275	0.828	-0.561	0.00
66.0413019781	101.2834715803	53.9337087795	66710948167949696	0.4906569578	66729635568719872	1.4555529447	65209079706818176	48.825	0.389	-0.921	0.00
66.7230110136	100.2920669768	52.7084100200	65175480179315840	1.1393416771	65190838982357760	1.1523691455	65007083101413888	50.246	0.417	-0.909	0.00
66.1038648468	101.3332108383	53.5434187569	65018417518780672	0.7183771997	65010519075247616	1.3733251145	65007083101413888	50.203	0.384	-0.923	0.00
69.6084689881	100.3871671152	53.6814218420	68152820227358720	0.5774252556	65125864716379264	2.4317915994	68298093201624960	49.391	0.416	-0.909	0.00

of the spatial distribution. This procedure has helped us both to locate some loops and the only void that appears and whose data comes from the "cycleLocation" attribute associated with the TDA function used.

After this geometrical-topological study, the density functions of specific physical parameters have been studied, differentiating the distributions in each of the two related components obtained. A series of graphs allow us to obtain a series of conclusions about differences that appear in both components for each parameter. HR-type diagrams have also been obtained showing interesting structures, in this case in 2D, that could be further investigated. However, our objective is not so ambitious, and we are satisfied with showing that, indeed, each connected component has different distributions for the same physical parameter. There are also differences in the distributions as a function of the distance from the center, for both connected components.

Finally, we have analyzed the possible influence of eliminating the 24 stars in our study. To do this, a table has been built in which, in addition to each of these 24 stars, the closest cc1 and cc2 stars appear, providing their identifiers and their distances in pc to the corresponding star. Likewise, the normalized proper motions and the radial velocity have been included. Some anomaly has been detected, and, in particular, there are only 3 stars out of the 24 that are between both components in a 1 pc wide band which separates them equidistantly. For none of these 3 stars, EDR3 provides its physical parameters. There are also anomalies in two other elements, which are closer to cc1: one with a proper motion of the opposite sign to that of the rest of the stars and another with a proper motion in declination that is also different from the rest. It is noteworthy that neither of the stars is provided physical values in the original source catalog. Leaving aside these three stars between both components, the remaining 21 can, without problems, be assigned to cc1 without changing any of the statistical values studied in the form of density or distribution functions in r. It is interesting to note that very few stars' data include the radial velocity value. We have also observed that the absence of astrophysical data is associated with the stars that prevented us from correctly detecting the two ccs. Hence, the associated distances probably contain a more significant margin of error.

Acknowledgements

This work has been partially supported by a grant UJI-B2021-15

References

[1] C.A.L. Bailer-Jones, J. Rybizki, M. Fouesneau, M. Demleitner, and R. Andrae, "VizieR Online Data Catalog: Distances to 1.47 billion stars in Gaia EDR3," *Astronomical Journal*, vol. 153, no. 6, article 206 (2021), DOI: 10.3847/1538-3881/abd806. Available: https://cdsarc.cds.unistra.fr/viz-bin/cat/I/352.

[2] B.T. Fasy, J. Kim, F. Lecci, C. Maria, D.L. Millman, and V. Rouvreau, "TDA: Statistical Tools for Topological Data Analysis," version 1.9 (2022). [Online]. Available: https://cran.r-project.org/web/packages/TDA/index.html.

[3] J.M. Converse and S.W. Stahler, "The dynamical evolution of the Pleiades," Monthly Notices of the Royal Astronomical Society, vol. 405, no. 1, pp. 666–680 (2010), DOI: 10.1111/j.1365-2966.2010.16505.x.

[4] R.M. Cutri, K. Deustua, E. I. Morales, R. L. M. C. Van Dyk, B. K. Hall, M. J. Skrutskie, and A. S. Law, "2MASS All-Sky Catalog of Point Sources," VizieR Online Data Catalog, II/246 (2003). [Online]. Available: https://irsa.ipac.caltech.edu/Missions/2mass.html.

[5] Gaia Collaboration (N. Brown, F. Altmann, H. L. D. R. Bonfils, J. B. Lindegren, M. de Bruijne, C. H. Holl, A. A. Adermann, P. Benatti, B. W. Harris, J. M. Robinson, and others), "VizieR Online Data Catalog: Gaia DR2," VizieR Online Data Catalog, I/345 (2018). [Online]. Available: https://cdsarc.cds.unistra.fr/viz-bin/cat/I/345. Original article DOI: 10.1051/0004-6361/201833051.

[6] Gaia Collaboration (N. Brown, F. Altmann, H. L. D. R. Bonfils, J. B. Lindegren, M. de Bruijne, C. H. Holl, A. A. Adermann, P. Benatti, B. W. Harris, J. M. Robinson, and others), "VizieR Online Data Catalog: Gaia EDR3," VizieR Online Data Catalog, I/350 (2020). [Online]. Available: https://vizier.cds.unistra.fr/viz-bin/VizieR-3?-source=I/350/. Original article DOI: 10.5270/esa-1ugzkg7.

[7] E. Høg, I. L. Lindegren, C. H. Roegiers, R. De Felice, P. M. L. Hainaut, P. J. Seitz, and S. J. Renner, "The Tycho-2 catalogue of the 2.5 million brightest stars," Astronomy and Astrophysics, vol. 355, pp. L27–L30 (2000). [Online]. Available: http://vizier.u-strasbg.fr/cgi-bin/VizieR-3?-source=I/259/tyc2.

[8] N. Lodieu, A. Pérez-Garrido, R. L. Smart, and R. Silvotti, "A 5D view of the α Per, Pleiades, and Praesepe clusters," *Astronomy and Astrophysics,* vol. 628, A66 (2019), DOI: 10.1051/0004-6361/201935533.

[9] C. Maria, “GUDHI, simplicial complexes and persistent homology packages,” (2014). [Online]. Available: http://gudhi.gforge.inria.fr/doc/latest/group__persistent__cohomology.html.

[10] D. Morozov, “Dionysus, a C++ library for computing persistent homology,” (2007). [Online]. Available: https://www.mrzv.org/software/dionysus/.

[11] S. E. Ragan, Th. Henning, J. Tackenberg, H. Beuther, K. G. Johnston, J. Kainulainen, and H. Linz, “Giant molecular filaments in the Milky Way,” *Astronomy and Astrophysics*, vol. 568, A73 (2014), DOI: 10.1051/0004-6361/201423401.

[12] M. F. Skrutskie, D. L. Shaya, R. H. Cutri, G. G. T. Athey, T. R. N. H. Kormendy, A. S. Law, and P. T. Evans, “The Two Micron All Sky Survey (2MASS),” *Astronomical Journal*, vol. 131, no. 2, pp. 1163-1183 (2006), DOI: 10.1086/498708. [Online]. Available: https://vizier.cds.unistra.fr/viz-bin/VizieR?-source=II/246.

[13] R. van de Weygaert, E. Platen, G. Vegter, B. Eldering, and N. Kruithof, “Alpha Shape Topology of the Cosmic Web,” in Proc. International Symposium on Voronoi Diagrams in Science and Engineering, Quebec, QC, Canada, pp. 224-234 (2010), DOI: 10.1109/ISVD.2010.24.

[14] VizieR catalogue access tool, “CDS, Strasbourg, France,” DOI: 10.26093/cds/vizier. The original description of the VizieR service was published in A&AS, vol. 143, pp. 23 (2000).

[15] Xin Xu, “SCHU.R,” (2018). [Online]. Available: https://github.com/xinxuyale/SCHU/tree/master.

[16] M. Zastrow, “Row reignites over distance of Pleiades star cluster,” Nature (2014), DOI: 10.1038/nature.2014.1578.